

Lawrence Berkeley National Laboratory

Recent Work

Title

STUDY OF ^{16}O , ^{20}Ne , ^{22}Ne , ^{28}Si , AND ^{32}S BY INELASTIC SCATTERING OF POLARIZED PROTONS

Permalink

<https://escholarship.org/uc/item/2mq068qg>

Authors

Swiniarski, R. de
Resmini, F.G.
Hendrie, D.L.
et al.

Publication Date

1975-08-01

Submitted to Nuclear Physics B

RECEIVED

LBL-2322 Rev. Preprint

SEP 11 1975

DEC 11 1975

LIBRARY

STUDY OF ^{16}O , ^{20}Ne , ^{22}Ne , ^{28}Si , AND ^{32}S
BY INELASTIC SCATTERING OF POLARIZED PROTONS

R. de Swiniarski, F. G. Resmini, D. L. Hendrie, and
A. D. Bacher

August 1975

Prepared for the U. S. Energy Research and
Development Administration under Contract W-7405-ENG-48

TWO-WEEK LOAN COPY

This is a Library Circulating Copy
which may be borrowed for two weeks.
For a personal retention copy, call
Tech. Info. Division, ~~Ext 5545~~



LBL-2322 Rev. c. 2

DISCLAIMER

This document was prepared as an account of work sponsored by the United States Government. While this document is believed to contain correct information, neither the United States Government nor any agency thereof, nor the Regents of the University of California, nor any of their employees, makes any warranty, express or implied, or assumes any legal responsibility for the accuracy, completeness, or usefulness of any information, apparatus, product, or process disclosed, or represents that its use would not infringe privately owned rights. Reference herein to any specific commercial product, process, or service by its trade name, trademark, manufacturer, or otherwise, does not necessarily constitute or imply its endorsement, recommendation, or favoring by the United States Government or any agency thereof, or the Regents of the University of California. The views and opinions of authors expressed herein do not necessarily state or reflect those of the United States Government or any agency thereof or the Regents of the University of California.

STUDY OF ^{16}O , ^{20}Ne , ^{22}Ne , ^{28}Si , AND ^{32}S
BY INELASTIC SCATTERING OF POLARIZED PROTONS[†]

R. de Swiniarski^{††}, F.G. Resmini^{*}, D.L. Hendrie, and A.D. Bacher^{**}

Lawrence Berkeley Laboratory
University of California
Berkeley, California 94720

June 1975

Abstract

Analyzing powers and cross sections have been measured for elastic and inelastic scattering of 24.5-MeV protons from ^{20}Ne and ^{22}Ne , and for ^{16}O , ^{28}Si , and ^{32}S at 30.3 MeV. The experimental results were analyzed in terms of the coupled-channels formalism using the rotational model and (for ^{32}S and ^{16}O) the vibrational model. The results for ^{20}Ne , ^{22}Ne , and ^{28}Si show a systematic trend of the hexadecapole deformation. Prolate shapes for ^{20}Ne and ^{22}Ne and an oblate shape for ^{28}Si are confirmed. The results for ^{32}S are almost equally well-reproduced by the vibrational or rotational model, and there is a slight preference for the prolate shape for this nucleus. The best fits for the analyzing power for all the nuclei were obtained by using the full Thomas form for the spin-orbit potential.

[†]Work supported under the auspices of the U.S. Atomic Energy Commission.

^{††}Present address: Institut des Sciences Nucléaires de Grenoble, France.

^{*}Present address: University of Milan, Italy.

^{**}Present address: Physics Department, University of Indiana, Bloomington, Indiana.

Key Words

Nuclear Reactions - ^{16}O , ^{20}Ne , ^{22}Ne , ^{28}Si , ^{32}S (\vec{p}, p')
measured $\sigma(\theta)$, $A(\theta)$. Optical model and coupled-channels analysis.
Deduced form of spin-orbit potential and deformation parameters.

1. Introduction

In the past several years, a large amount of proton elastic and inelastic analyzing power data¹⁻⁴⁾ has become available, arising from the increase in number and improvement in quality of polarized beam facilities. Analysis of the analyzing power data with distorted-wave Born approximation (DWBA) codes or with coupled-channels (CC) methods have been reasonably successful for collective 2^+ or 3^- levels for several nuclei in the $f_{7/2}$ shell, $g_{9/2}$ shell, and s-d shell¹⁾. In order to obtain good fits in the macroscopic treatment, it was found necessary to deform the real, imaginary, and spin-orbit terms in the form factor. Different ways of deforming the spin-orbit potential have been used¹⁾, but have led to almost equivalent results. These models were unable, however, to reproduce the large asymmetries observed for the transitions to the first 2^+ states in ^{54}Fe and ^{52}Cr ¹⁾. The deformed spin-orbit potential which has been previously used in the framework of the macroscopic collective model was essentially phenomenological, having a form proportional to the radial derivative of the spin-orbit term of the optical potential¹⁾. Problems have also appeared in the attempt to describe the data with microscopic models. Applications of the microscopic model to these states have usually produced poor agreement with experiment^{1-3, 5, 6)}.

More recently, Sherif and Blair introduced the concept of the "full Thomas Form" of the spin-orbit potential in the DWBA collective model formalism⁷⁾. Considerable improvements to the fits, especially

at forward angles, were immediately observed⁷). Such a deformed spin-orbit term has now been included by Raynal in a coupled-channels (CC) program⁸). Calculations will be presented here (some of them have already been partly published elsewhere⁹) for the analyzing powers obtained by inelastic scattering of 24.5-MeV polarized protons from the strongly excited low-lying states in ^{20}Ne and ^{22}Ne , and of 30.3-MeV polarized protons for the collective states in ^{16}O , ^{28}Si , and ^{32}S . Part of the purpose of this work was to test the possible improvements in the CC analysis produced by the use of the Sherif-Blair form of the spin-orbit interaction.

A second goal of the experiments was to investigate the nuclear structure of the target nuclei. Recent coupled-channels calculations¹⁰) have shown the existence of a large Y_4 deformation in the $K=0^+$ band in ^{20}Ne , and suggest the possible existence of such hexadecapole deformation in other s-d shell nuclei. Moreover, because recent (α, α') ¹¹) or $(^3\text{He}, ^3\text{He}')$ ¹²) experiments have yielded large differences in the evaluation of the Y_4 deformation of s-d shell nuclei, polarization experiments can provide additional information for a more precise determination of the deformations. The rotational model provides a reasonably accurate description of the low-lying levels in some s-d shell nuclei, for instance ^{20}Ne and ^{28}Si , but the situation is less clear for ^{32}S . We had originally hoped that analyzing power measurements would allow a clear distinction between rotational and vibrational models for the low-lying states of ^{32}S , but this was found not to be so.

Since cross-section data for inelastic proton scattering on ^{20}Ne at 24.5 MeV¹³⁾ and on ^{28}Si ¹⁴⁾ and ^{16}O ¹⁵⁾ at 30.3 MeV were already available, emphasis was concentrated on the measurement of the analyzing power. Cross sections for $^{22}\text{Ne}(p,p')$ and $^{32}\text{S}(p,p')$ were obtained simultaneously with the polarization data and are therefore somewhat less precise.

After a brief description of the experimental method in sec. 2, the analyzing power data for ^{16}O , ^{20}Ne , ^{22}Ne , ^{28}Si , and ^{32}S are presented in sec. 3. The discussion of the optical model analysis for the different nuclei is made in sec. 4, while sec. 5 discusses the coupled-channels calculations using various spin-orbit distortions and deformations. A short summary of the conclusions is given in sec. 6.

2. Experimental Method

The experiments were performed using the Berkeley 88" cyclotron and polarized ion source¹⁶⁾. The source is of the atomic beam type and uses an adiabatic rf transition and strong field ionizer. The polarized-ion beam is injected axially¹⁷⁾ into the center of the cyclotron and deflected into a proper orbit by a gridded electrostatic mirror. During these experiments, up to 60 nA of beam were delivered onto the target with an average polarization of about 75%. The beam polarization was monitored continuously with a standard ^{12}C polarimeter¹⁸⁾, which was subsequently calibrated by accurate p- ^4He polarization measurements at the same energy¹⁹⁾. The beam intensity was continuously monitored with a pair of Si(Li) detectors placed symmetrically at 45 degrees with respect to the beam direction and was checked periodically with a Faraday cup. The thick polarimeter target precluded the continuous use of a Faraday cup.

The data were taken with eight 5-mm-thick Si(Li) detectors cooled by thermoelectric devices to about -25°C . In order to measure asymmetries, the counters were arranged in symmetric pairs to the left and right of the beam direction. In addition, the beam polarization was manually reversed at the source by inverting the magnetic field of the ionizer halfway through each data-taking run. This redundancy of asymmetry measurements allowed us to eliminate many sources of systematic error, such as those due to uncertainties in counter apertures, slight misalignments of the beam, and differential counting-rate effects in the detectors and in the polarimeter²⁰⁾.

The analyzing powers, A, were obtained with the use of the formula

$$A = \frac{1}{P} \frac{r - 1}{r + 1},$$

where

$$r = \left(\frac{L^+ \times R^-}{L^- \times R^+} \right)^{1/2}, \text{ and}$$

where P is the measured average beam polarization, L and R designate the number of paired counts accumulated in the left and right counters with respect to the beam direction, and the superscripts + and - refer to data accumulated with the incident beam polarized in the spin up and spin down directions, respectively.

The ^{28}Si target was a slightly enriched ($\geq 95\%$), self-supporting foil of $\sim 400 \mu\text{g}/\text{cm}^2$ thickness. Data for ^{32}S and ^{16}O were taken simultaneously using a SO_2 gas target. The neon gas targets were filled with isotopes enriched to $> 99.9\%$ for ^{20}Ne and $\geq 95\%$ for ^{22}Ne . All gas targets were operated at about 20 cm Hg pressure, which was measured, along with the temperature, before and after each run. The overall energy resolution was about 180 keV for the gas-target data and about 150 keV for the ^{28}Si data, the latter being mostly due to the energy spread of the incident beam. Except for the 3^- , 1^- doublet in ^{20}Ne at 5.7 MeV, and the 2^+ , 4^+ doublet in ^{32}S at 4.4 MeV, all low-lying strongly excited states of the s-d shell nuclei were clearly separated.

3. Experimental Results

The measured analyzing powers for the low-lying excited states in ^{20}Ne and ^{22}Ne are shown in figs. 1 and 2; the data were taken with an incident beam energy of 24.5 MeV. These two figures exhibit the similarities that exist for the lowest 0^+ and 2^+ states in ^{20}Ne and ^{22}Ne . Moreover, cross sections to the 0^+ and 2^+ states in ^{20}Ne and ^{22}Ne , to be seen in later figures, are also very similar at our energy and at higher energy²¹). This is not the case for the 4^+ states in ^{20}Ne and ^{22}Ne , where large differences exist between the two analyzing powers as well as between the two cross sections. It is also worthwhile to point out the large difference between the analyzing power for the first and second 2^+ states in ^{22}Ne (fig. 2). Such a large difference has already been observed in the $f_{7/2}$ shell¹), and its presence suggests the need for a microscopic interpretation. Figure 3 shows the analyzing power for the $K=0^+$ rotational band in ^{28}Si , together with the strongly excited 0^+ , 2^+ , and 3^- states in ^{32}S , while fig. 4 presents the analyzing power for several states in ^{16}O . The data presented in figs. 3 and 4 were taken at an energy of 30.3 MeV. Here also a striking difference can be seen between the 2^+ curves in fig. 3. The first bump on the ^{32}S curve at 50° is much lower than in the corresponding curve of ^{28}Si and resembles the shape of the analyzing power taken at 20.3 MeV for ^{24}Mg ¹). The analyzing powers for the 0^+ (g.s.) and 2^+ state in ^{28}Si and for the 0^+ (g.s.) in ^{16}O are in good agreement with other recent data¹).

The error bars shown on the figures reflect only statistical errors unless the levels were difficult to resolve, in which case the errors were increased appropriately. Most of the integrated counts were obtained from the spectra with a peak-fitting program and were checked for internal consistency.

4. Optical Model Analysis

Since ^{20}Ne and ^{22}Ne are strongly deformed, only preliminary optical model parameters needed for the CC calculation can be obtained from an optical model search. In their analysis of α -scattering in the rare earth region, Hendrie et al.²²⁾ obtained good fits for the rotational band cross sections by first deriving optical model parameters from a nearly spherical nucleus and then using these parameters in a coupled-channels calculation for the deformed nuclei. Such an attempt has been made by trying to use the optical model parameters obtained from an analysis of the elastic cross section and polarization data of ^{16}O taken from the literature²³⁾, but this has failed completely to describe the excited states of ^{20}Ne . Instead we obtained a starting set of optical model parameters from a multi-parameter search using the elastic scattering data, and then adjusted the parameters so as to preserve the fits to the elastic scattering in the coupled-channels calculations. For ^{20}Ne and ^{22}Ne , it was found that only slight adjustments of W_D , a_I , V_0 and a_0 were needed; no changes were required for the other nuclei.

Table 1 lists the best-fit parameters obtained from a search on all parameters. The corresponding fits to the elastic cross sections and polarizations are shown in fig. 5. Most of the optical model calculations were carried out with the code MAGALI²⁴⁾. The searches included an adjustment for the absolute normalization of the cross sections; the weights given each data point included only statistical errors for

cross sections and polarizations. The calculated cross sections and analyzing powers were averaged over the finite angular acceptance of the detectors during the search. The curves shown in the figs, however, do not include this averaging.

The data for ^{16}O , ^{28}Si , and ^{32}S were taken at an energy of 30.3 MeV with the same experimental equipment described in sec. 2. Because for ^{16}O and ^{28}Si only analyzing powers were obtained during these experiments, calculations were carried out using the elastic cross sections of ref. ²³⁾ for ^{16}O and of ref. ¹⁴⁾ for ^{28}Si ; cross sections for the 0^+ , 2^+ , and 3^- states in ^{32}S were obtained simultaneously with the analyzing powers. Very good fits were obtained for these three nuclei as shown in figs. 6 and 7. The corresponding parameters are presented in Table 1. A fit to the ^{32}S elastic-analyzing power could be obtained only with a very small spin-orbit radius and a comparably large spin-orbit diffuseness.

Several general conclusions can be drawn from the optical model analysis for the s-d shell nuclei. We find a smaller radius (average around 1.07 fm) and a larger diffuseness (average value around 0.73 fm) than have previously been ascribed to the real potential. The imaginary radius remains constant around 1.33 fm, about 20% larger than the real radius. The spin-orbit potential is both smaller by 20% and less diffuse (except for ^{32}S) than those of the real central well. These trends have already been noted in a review paper on this subject²⁵⁾ for heavier nuclei, but it is interesting that they are also valid for light nuclei. Searches including volume absorption terms made no significant effect.

5. Coupled Channels Calculations

The spectrum of excited states in most nuclei in the 2s-1d shell exhibits a rotational character²⁶⁾ indicative of a permanent deformation. The large static quadrupole moments for the first excited states²⁷⁾ and the results of Hartree-Fock and Hartree-Fock-Bogoliubov type calculations²⁸⁾ also characterize the s-d shell as a region of permanent ground-state deformation. Some of these calculations suggest that some nuclei in this region should also have a ground-state hexadecapole deformation, which changes both size and sign through the shell, together with the quadrupole deformation²⁹⁻³¹⁾. Data from the inelastic scattering of protons¹⁰⁾ and alpha particles¹¹⁾ on ^{20}Ne , analyzed in the coupled-channels formalism, have shown that a large hexadecapole deformation (β_4) was needed to reproduce both the shape and the magnitude of the cross sections leading to the lowest 2^+ , 4^+ , and 6^+ states in ^{20}Ne .

Similar analyses^{10,11)} of other inelastic scattering data in the s-d shell has shown that the Y_2 and Y_4 moments vary considerably throughout this region. Nevertheless, considerable differences in the value of the hexadecapole deformation β_4 , especially in the case of ^{20}Ne , were obtained, depending upon the type of particles used in the scattering experiments^{10-12,32,33)}. The additional information provided by analyzing power measurements has been shown to be helpful in resolving such ambiguities^{9,34)}.

The strong couplings between states of the ground-state rotational band required the use of the coupled-channels (CC) reaction formalism

in order to treat adequately the multiple paths of excitation to the excited states³⁵). In this formalism, the intrinsic deformation of the members of the $K = 0$ rotational band is parametrized according to the following definition of the nuclear radius:

$$R(\theta) = R_0 [1 + \beta_2 Y_{20}(\theta) + \beta_4 Y_{40}(\theta)]$$

The interaction potential arises from the deformation of the real and imaginary central potentials, the spin-orbit potential, and the Coulomb potential. The various multiple-excitation paths between the coupled states are explicitly included, assuming pure rotational matrix elements between them. Coulomb excitation was always included but never showed significant effects. All expansions are carried to convergence, so that the only approximations are in the nuclear model and those inherent in the CC formalism³⁵).

5.1 COUPLED-CHANNELS CALCULATIONS: ^{20}Ne AND ^{22}Ne

Previously reported CC calculations^{9,10}) on ^{20}Ne , which used a simplified symmetrized form (phenomenological) of the deformed spin-orbit potential¹), failed to reproduce even the shape of the observed analyzing powers for the 2^+ and 4^+ states in ^{20}Ne . Recent calculations have shown that the fits to analyzing power data for less strongly coupled nuclei can be significantly improved when the full Thomas form of Sherif and Blair for the deformed spin-orbit potential is used⁷). This full Thomas form has been introduced by J. Raynal in a coupled-channels program using a sequential iteration technique to handle the additional

complexity of this potential⁸) (Program ECIS 71). The results of such calculations for ^{20}Ne are shown in fig. 8. The CC calculations reproduce well the measured analyzing power when the full Thomas term is used. The curve with $\beta_4 = 0.0$ shows the pronounced sensitivity of the analyzing power of the 2^+ and 4^+ states to the Y_4 deformation. The third curve shows that CC calculations using the simplified symmetrized form of the deformed spin-orbit potential result in a poor fit. The corresponding CC cross-sections calculations, also presented in fig. 8, show the sensitivity to the β_4 deformation even for the 0^+ (g.s.). On the other hand, cross sections are insensitive to the detailed form of the spin-orbit potential and therefore only calculations using the full Thomas form are presented. While the value obtained for β_2 for ^{20}Ne is in relatively good agreement with results from alpha scattering^{11,12}), our value for β_4 appears to be a factor of 2 larger, well outside quoted errors, even when the deformation values are linearly scaled to account for the different radii³⁶). Our results are in better agreement with electron scattering results³³).

Recently J. Raynal has performed a coupled-channels calculation (using a new program that includes a search routine) on the ^{20}Ne data³⁷). By letting all parameters vary, including the β_2 and β_4 deformations, and doing a search on all cross sections and analyzing powers for the 0^+ , 2^+ , and 4^+ in ^{20}Ne , the calculations yield final β_2 and β_4 deformations equal to 0.42 and 0.27 respectively. The optical model parameters were almost unchanged except for the spin-orbit diffuseness, which reduced to ~ 0.10 fm.

The CC results for the lowest 0^+ , 2^+ , and 4^+ states in ^{22}Ne are given in fig. 9. We see that the cross sections as well as the analyzing powers favor a rather small value for the Y_4 deformation ($\beta_4 = 0.05$) of ^{22}Ne , while the value found for β_2 is similar to that for ^{20}Ne . Similar conclusions have also been obtained from 40-MeV proton scattering work on ^{20}Ne and $^{22}\text{Ne}^{21}$, as well as from alpha scattering experiments¹¹⁾.

Figure 9 shows again that the calculations strongly support the full Thomas form and that the analyzing powers for the 0^+ , 2^+ , and 4^+ states are very well reproduced. It has been suggested on a theoretical basis⁷⁾ that the spin-orbit deformation is greater than that of the central potential. Following this suggestion in the case of ^{20}Ne and ^{22}Ne , we find the best fits for the analyzing power were obtained when the ratio of the two deformations was taken to be 2. Comparison between microscopic and macroscopic treatments by Raynal⁸⁾ indicates that this ratio is directly related to the nuclear structure of the excited states and hence some variations may be expected throughout the s-d shell. However, no calculations have yet been performed to predict the size of the effect for ^{20}Ne and ^{22}Ne . As will be seen later, good fits for ^{32}S and ^{28}Si can be obtained without having to increase the deformation of the spin-orbit potential with respect to the central potential.

5.2 COUPLED-CHANNELS CALCULATIONS: ^{16}O , ^{28}Si , AND ^{32}S

Previous CC calculations done on the 17.5-MeV proton inelastic scattering data of Crawley¹⁰⁾ have used oblate shapes with large hexadecapole moments ($\beta_4 = 0.25$) for ^{28}Si and ^{32}S . Even if the rotational


character of the ^{28}Si lowest 0^+ , 2^+ , 4^+ states is well established^{38,39}) and the oblate shape confirmed^{19,41}), the situation for ^{32}S is much more complicated³⁹). Recent measurements of the quadrupole moments of the first excited states of even-even nuclei in the 2s-1d shell²⁷) brought additional evidence for the oblate shape for ^{28}Si ($Q_0 < 0$). The surprising change in sign of Q_0 between ^{28}Si and ^{32}S appears to indicate a serious difficulty in predicting deformations of nuclei in this mass region. Several recent experiments have suggested that the levels of ^{32}S up to an excitation of 5 MeV are well explained on the assumption that ^{32}S is an almost spherical vibrational nucleus³³⁻⁴¹). Since a recent α - γ angular correlation experiment⁴²) on ^{28}Si and a (α, α') experiment⁴³) on ^{32}S yields very surprising prolate ($\beta_2 > 0$) quadrupole deformation for these nuclei, it appears necessary to analyze these data both with the vibrational model and with the rotational model with oblate and prolate deformations.

The CC calculations for the $K = 0^+$ ground state band (2^+ and 4^+ states) of ^{28}Si using both the vibrational model and the rotational model (prolate shape) are presented in fig. 10. Although the full Thomas form was used, the agreement with the data is poor. The CC-calculations results using the full Thomas term and rotational (oblate deformation) are presented in fig. 11. Very good fits to cross sections and polarizations are obtained with a negative quadrupole deformation $\beta_2 = -0.40$ and a positive hexadecapole β_4 deformation equal to $+0.10$. The values of these deformations are quite different from those previously determined¹⁰) using only the Crawley cross sections, but are

in very good agreement with the (α, α') ¹¹⁾ and (e, e') ³³⁾ results and with microscopic α -cluster model calculations³¹⁾, as well as with some recent polarization data at 25.25 MeV⁴⁴⁾. Fig. 11 also shows the sensitivity of the theory to the β_4 deformation parameter. If β_4 is increased beyond 0.1, the fit deteriorates quite rapidly. Since no cross sections for the 4^+ state in ^{28}Si were available, the value determined for the β_4 deformation is less precise; an error of ± 0.04 is assigned to the β_4 determined in ^{28}Si . In addition, fig. 11 shows the results when $\beta_{\text{so}}/\beta_{\text{central}}$ was equal to unity, compared to the case where the deformation lengths $(\beta_{\text{LS}} r_{\text{LS}}/\beta_{\text{central}} r_0)$ were equal to unity. In the latter case, $\beta_{\text{LS}}/\beta_{\text{central}}$ is equal to 1.29. Even better fits could be obtained by increasing the ratio up to 1.5⁴⁴⁾, or to 2.0 as for ^{20}Ne , but the optimum value of β_4 did not change significantly.

Coupled-channels calculations for ^{32}S are presented using either the rotational model (fig. 12) or the vibrational model (fig. 13). As seen in fig. 12, it is quite difficult to distinguish between oblate and prolate deformation. The overall χ^2 slightly favors a prolate shape for ^{32}S ($\beta_2 > 0$), but when only polarization data are taken into account, the oblate solution is slightly better ($\beta_2 = -0.30$). Therefore, an assignment of the sign of the deformation for ^{32}S is not possible on the basis of our data. Addition of a hexadecapole deformation β_4 to the quadrupole deformation β_2 has little effect if β_4 is small (up to around 0.1), but it quickly destroys the fits to the data when it is

increased above this value. Therefore we conclude that the hexadecapole deformation is absent or very small in the ground state band of ^{32}S .

Fig. 13 presents CC results using a vibrational model with either $0^+, 2^+$ coupling and a deformation parameter of +0.3 for the 2^+ , or a $0^+, 2^+$, and 3^- coupling with a deformation for the 3^- equal to +0.41. The fits to the data are quite good, especially in the case of the $(0^+, 2^+)$ coupling; they are essentially equivalent to those of the rotational model.  It has been suggested from recent experiments such as $(p,p')^{41)}$, $(d,d')^{33)}$ or by lifetime measurements⁴⁵⁾ that the upper half of the s-d shell nuclei may have a spherical structure, although this behavior is not reproduced by Hartree-Fock calculations³⁰⁾. The energy level spacings of ^{32}S indeed show considerable deviation from the rotational model pattern and more resemble a vibrational spectrum. From our data and analysis, it is impossible to choose between rotational or vibrational structure. More precise data, especially for the 4^+ states at 4.47 MeV or for the next $0^+, 2^+, 4^+$ states which may be the two phonon states in the vibrational model, are needed.

Finally, the results of CC calculations for the 2^+ states at 6.92 MeV and the 3^- state at 6.13 MeV for ^{16}O are presented in fig. 14. Very good fits for 3^- state and an acceptable fit for the 2^+ state for this nucleus are obtained in the framework of the collective vibrational model with the full Thomas form and a deformation parameter of +0.50 for the 3^- and 0.2 for the 2^+ .

6. Conclusions

In summary, coupled-channels calculations using permanently deformed nuclear wave functions reproduce well our cross section and analyzing power data on the elastic and inelastic scattering of polarized protons exciting the ground state rotational bands of ^{20}Ne , ^{22}Ne , and ^{28}Si . Table 3 summarizes the nuclear deformation determined from the CC calculations. Prolate shapes of ^{20}Ne and ^{22}Ne and an oblate shape of ^{28}Si are strongly preferred. The situation for ^{32}S is not clear, since the calculations could not distinguish between oblate-prolate deformation or for a spherical vibrational structure, although the overall best χ^2 slightly favors a prolate deformation.

Hexadecapole deformations found for ^{22}Ne and ^{28}Si are in good agreement with recent $(\alpha, \alpha')^{11}$, $(e, e')^{33}$ experiments and with theoretical calculations³¹). Large differences for the Y_4 moment of ^{20}Ne appear in the literature, especially in scattering experiments using α or ^3He particles as probes^{11, 12}).

Finally, we have shown over a wide range of nuclei that the use of the Blair-Sherif form for the deformed spin-orbit interaction, in conjunction with a coupled-channels reaction calculation, is necessary to explain our cross-section and analyzing power results. However, we are gratified that calculations of the deformation parameters using simple forms of the interaction do not greatly change the results.

We would like to thank Dr. A.U. Luccio for assistance in the operation of the polarized source and Drs. J. Sherman and G.R. Plattner for their help during the course of this experiment. We are especially grateful to Dr. H.E. Conzett and Dr. B.G. Harvey for their assistance and support.

References

- 1) G.R. Satchler, Proc. 3rd Int. Symp. on Polarization Phenomena in Nuclear Reactions, Madison 1970, ed. H.H. Barschall and W. Haeberli (The University of Wisconsin Press, Madison, 1971) p. 155, and references therein
- 2) C. Glashausser and J. Thirion, Advances in Nucl. Phys. 2 (1969) 79
- 3) J. Lowe, Nucl. Phys. A162 (1971) 438
- 4) Polarization Phenomena in Nuclear Reactions, Proc. 3rd Int. Symp. on Polarization Phenomena in Nuclear Reactions. Madison 1970, ed. H.H. Barschall and W. Haeberli (and references therein)
- 5) J.L. Escudié, A. Tarrats and J. Raynal, ibid., p. 705
- 6) P.D. Greaves, V. Hnizdo, J. Lowe and O. Karban, ibid., p. 697; and Nucl. Phys. A179 (1972) 1
- 7) H. Sherif and J.S. Blair, Nucl. Phys. A140 (1970) 33 and references quoted therein
- 8) J. Raynal, Proc. Symp. on Nuclear Reactions Mechanisms and Polarizations Phenomena, Laval University, Quebec 1969, p. 75
- 9) R. de Swiniarski, A.D. Backer, F.G. Resmini, G.R. Plattner, D.L. Hendrie and J. Raynal, Phys. Rev. Lett. 28 (1972) 1139
- 10) R. de Swiniarski, C. Glashausser, D.L. Hendrie, J. Sherman, A.D. Bacher and E.A. McClatchie, Phys. Rev. Lett. 23 (1969) 317

- 11) J. Specht, H. Rebel, G. Schatz, G.W. Schweimer, G. Hauser, and R. Löhken, Nucl. Phys. A143 (1970) 373; H. Rebel, G.W. Scheimer, G. Schatz, J. Specht, R. Löhken, G. Hauser, D. Habs, and H. Klewe-Nebenius, Nucl. Phys. A182 (1972) 145; J.W. Frickey, K.A. Eberhard and R.H. Davis, Phys. Rev. C4 (1971) 434
- 12) K.W. Kemper, D.S. Haynes and N.R. Fletcher, Phys. Rev. C4 (1971) 408
- 13) R. de Swiniarski, J. Sherman, A.D. Bacher, C. Glashausser, D.L. Hendrie and E.A. McClatchie, Bull. Am. Phys. Soc. 14 (1969) 531
- 14) H.S. Sandhu, J.M. Cameron and W.F. McGill, Nucl. Phys. A169 (1971) 600; H.S. Sandhu, private communication; R.K. Cole, C.N. Waddell, R.R. Ditman and H.S. Sandhu, Nucl. Phys. 75 (1969) 241
- 15) J.K. Dickens, D.A. Haner and C.N. Waddell, Phys. Rev. 129 (1963) 743; *ibid.* 132 (1963) 2159
- 16) A.U. Luccio, D.J. Clark, D. Elo, P. Frazier, D. Morris and M. Renkas, IEEE Trans. Nucl. Sci. NS-16 (1969) 110
- 17) D.J. Clark, A.U. Luccio, F.G. Resmini and H. Meiner in Proc. 5th Int. Cyclotron Conf., Oxford (England), (Butterworth, London 1971) p. 610
- 18) R.M. Craig, J.C. Dore, G.W. Greenlees, J.S. Lilley, J. Lowe and P.C. Rowe, Nucl. Instrum. Methods 30 (1964) 269
- 19) A.D. Bacher, G.R. Plattner, H.E. Conzett, D.J. Clark, H. Grunder and W.F. Tivol, Phys. Rev. C5 (1972) 1147
- 20) G.G. Ohlsen and P.W. Keaton, Nucl. Instrum. Methods 109 (1973) 41

- 21) D. Madland and N.M. Hintz, J.H. Williams Laboratory, Annual Report 1970, University of Minnesota, p. 23
- 22) D.L. Hendrie, N.K. Glendenning, B.G. Harvey, O.N. Jarvis, H.H. Duhm, J. Saudinos and J. Mahoney, Phys. Lett. 26B (1968) 127; N.K. Glendenning, D.L. Hendrie and O.N. Jarvis, Phys. Lett. 26B (1968) 131
- 23) J.M. Cameron, J.R. Richardson, W.T.H. Van Oers and J.W. Verba, Phys. Rev. 167 (1968) 908
- 24) J. Raynal, "MAGALI" DPh.T/69-42, Saclay
- 25) G.R. Satchler, Nucl. Phys. A92 (1967) 273
- 26) H.E. Gove, University of Rochester Report UR.NSRL-7 (1968) and references therein
- 27) O. Häusser, B.W. Hooten, D. Pelte, T.K. Alexander and H.C. Evans, Phys. Rev. Lett. 22 (1969) 359; D. Pelte, O. Häusser, T.K. Alexander and H.C. Evans, Can. J. Phys. 47 (1969) 1929; K. Nakai, J.L. Quebert, F.S. Stephens and R. Diamond, Phys. Rev. Lett. 24 (1970) 903
- 28) S. Das Gupta and M. Harvey, Nucl. Phys. A94 (1967) 602; B. Castel and J.P. Sennen, Nucl. Phys. A127 (1969) 141
- 29) C. Brihaye and G. Reidemeister, Nucl. Phys. A100 (1967) 65; H.G. Benson and B.H. Flowers, Nucl. Phys. A126 (1969) 305; M.K. Pal and A.P. Stamp, Phys. Rev. 158 (1967) 924
- 30) A.L. Goodman, G.L. Struble, J. Bar-Touv and A. Goswami, Phys. Rev. C2 (1970) 380

- 31) Y. Abgrall, B. Morand and E. Caurier, Nucl. Phys. A192 (1972) 372;
Y. Abgrall, private communication
- 32) D.K. Olsen, T. Udagawa, T. Tamura and R.E. Brown, Phys. Rev. C8
(1973) 608
- 33) Y. Horikawa, Y. Torizuka, A. Nakada, S. Mitsunobu, Y. Kojima and
M. Kimura, Phys. Lett. 36B (1971) 9
- 34) M.P. Barbier, R. Lombard, J.M. Moss and Y. Terrien, Phys. Lett.
34B (1971) 386
- 35) N.K. Glendenning in International School of Physics Enrico Fermi,
Course XL (Academic Press, New York, 1967)
- 36) D.L. Hendrie, Phys. Rev. Lett. 31 (1973) 478
- 37) J. Raynal, private communication
- 38) M.M. Aleonard, D. Castera, P. Hubert, F. Leccia, P. Menrath and
J.P. Thibaud, Nucl. Phys. A146 (1970) 90
- 39) M.C. Mermaz, C.A. Whitten, Jr. and D.A. Bromley, Phys. Rev. 187
(1969) 1466
- 40) J.P. Thibaud, M.M. Aleonard, D. Castera, P. Hubert, F. Leccia and
P. Menrath, Nucl. Phys. A135 (1969) 281
- 41) R. Lombard, H. Kamitsubo, J. Raynal and J. Gosset, Compt. Rend.
Ac. Sc., Paris, 274 (1972) Serie B, 761

- 42) C.E. Ahlfeld, G.E. Assousa, R.A. Lasalle, W.J. Thomson, H.A. Van Ruisvelt and N.P. Heydenburg, Nucl. Phys. A191 (1972) 137
- 43) G.W. Schweimer, H. Rebel, G. Nowicki, G. Hauser and R. Löhken, Phys. Lett. 39B (1972) 627
- 44) R. de Swiniarski, H.E. Conzett, C.R. Lamontagne, B. Frois and R.J. Slobodrian, Can. J. Phys. 51 (1973) 1293
- 45) G.T. Garvey, K.W. Jones, L.E. Carlson, D.A. Hutcheon, A.G. Robertson and D.F.H. Start, Nucl. Phys. A160 (1971) 25

Table 1

Optical parameters obtained in optical model search.

Nucleus	Search	V_0 (MeV)	r_0 (fm)	a_0 (fm)	W_V (MeV)	W_D (MeV)	r_I (fm)	a_I (fm)	V_{LS} (MeV)	r_{LS} (fm)	a_{LS} (fm)	χ_G^2	χ_P^2
^{20}Ne	$\sigma + p$	59.10	1.01	0.77	0.0	7.54	1.26	0.62	3.57	0.86	0.33	217	1290
^{22}Ne	$\sigma + p$	58.0	1.05	0.78	0.0	7.73	1.33	0.57	3.95	0.88	0.31	31	562
^{28}Si	$\sigma + p$	50.72	1.11	0.68	0.0	6.10	1.34	0.54	6.43	0.86	0.55	261	150
^{32}S	$c + p$	53.87	1.09	0.73	0.0	6.3	1.34	0.63	7.30	0.74	0.91	84	98
^{16}O	$c + p$	43.25	1.14	0.69	0.0	2.78	1.36	0.84	4.31	1.11	0.45	855	135

Table 2
Optical parameters used in coupled-channels calculations.

Nucleus	V_o (MeV)	r_o (fm)	a_o (fm)	W_V (MeV)	W_D (MeV)	r_I (fm)	a_I (fm)	V_{LS} (MeV)	r_{LS} (fm)	a_{LS} (fm)
^{20}Ne	59.0	1.01	0.75	0.0	6.5	1.26	0.55	3.57	0.90	0.33
^{22}Ne	57.0	1.05	0.75	0.0	6.3	1.33	0.55	3.95	0.88	0.31
^{28}Si	50.72	1.11	0.68	0.0	6.10	1.34	0.54	6.43	0.86	0.55
^{32}S	53.87	1.09	0.73	0.0	6.3	1.34	0.63	7.30	0.74	0.91
^{16}O	43.25	1.14	0.69	0.0	2.78	1.36	0.84	4.31	1.11	0.45

Table 3

Values of deformation parameters and multipole moments from scattering of polarized protons

	^{20}Ne	^{22}Ne	^{28}Si	^{32}S
β_2	+0.47	+0.47	-0.40	(+)0.30
β_4	+0.28	+0.05	+0.10	-

Figure Captions

- Figure 1 Measured analyzing powers (A) for low-lying excited states in ^{20}Ne obtained by scattering of 24.5-MeV protons.
- Figure 2 Measured analyzing powers (A) for the strongly excited states in ^{22}Ne obtained by scattering of 24.5-MeV protons.
- Figure 3 Measured analyzing powers (A) for low-lying collective states in ^{28}Si and ^{32}S obtained by scattering of 30.3-MeV protons.
- Figure 4 Measured analyzing powers (A) for several states in ^{16}O obtained by scattering of 30.3-MeV protons.
- Figure 5 Optical model predictions for the elastic cross sections and analyzing powers for ^{20}Ne and ^{22}Ne . The parameters are those of Table 1.
- Figure 6 Optical model predictions for the elastic cross sections and analyzing powers for ^{28}Si and ^{32}S . Parameters of Table 1 are used.
- Figure 7 Optical model prediction for the elastic cross section and analyzing power for ^{16}O . The parameters of Table 1 are used.
- Figure 8 Coupled-channels calculations (rotational model) for the measured analyzing powers and cross sections for the first 0^+ , 2^+ , and 4^+ states in ^{20}Ne with and without the full Thomas form. Optical model parameters of Table 2 are used. CC calculations with full Thomas form: — $\beta_2 = 0.47$, $\beta_4 = 0.28$; — · — $\beta_2 = 0.47$, $\beta_4 = 0.0$; --- CC calculations with limited spin-orbit form where $\beta_2 = 0.47$, $\beta_4 = 0.28$.

Figure 9 Measured analyzing powers and cross sections for the first 0^+ , 2^+ , and 4^+ states in ^{22}Ne with some coupled-channels calculations (rotational model) with and without the full Thomas form. Optical model parameters of Table 2 were used. CC calculations with full Thomas form: — $\beta_2 = 0.47$, $\beta_4 = 0.05$; --- $\beta_2 = 0.47$, $\beta_4 = 0.00$; — · — CC calculations with limited spin-orbit where $\beta_2 = 0.47$, $\beta_4 = 0.05$.

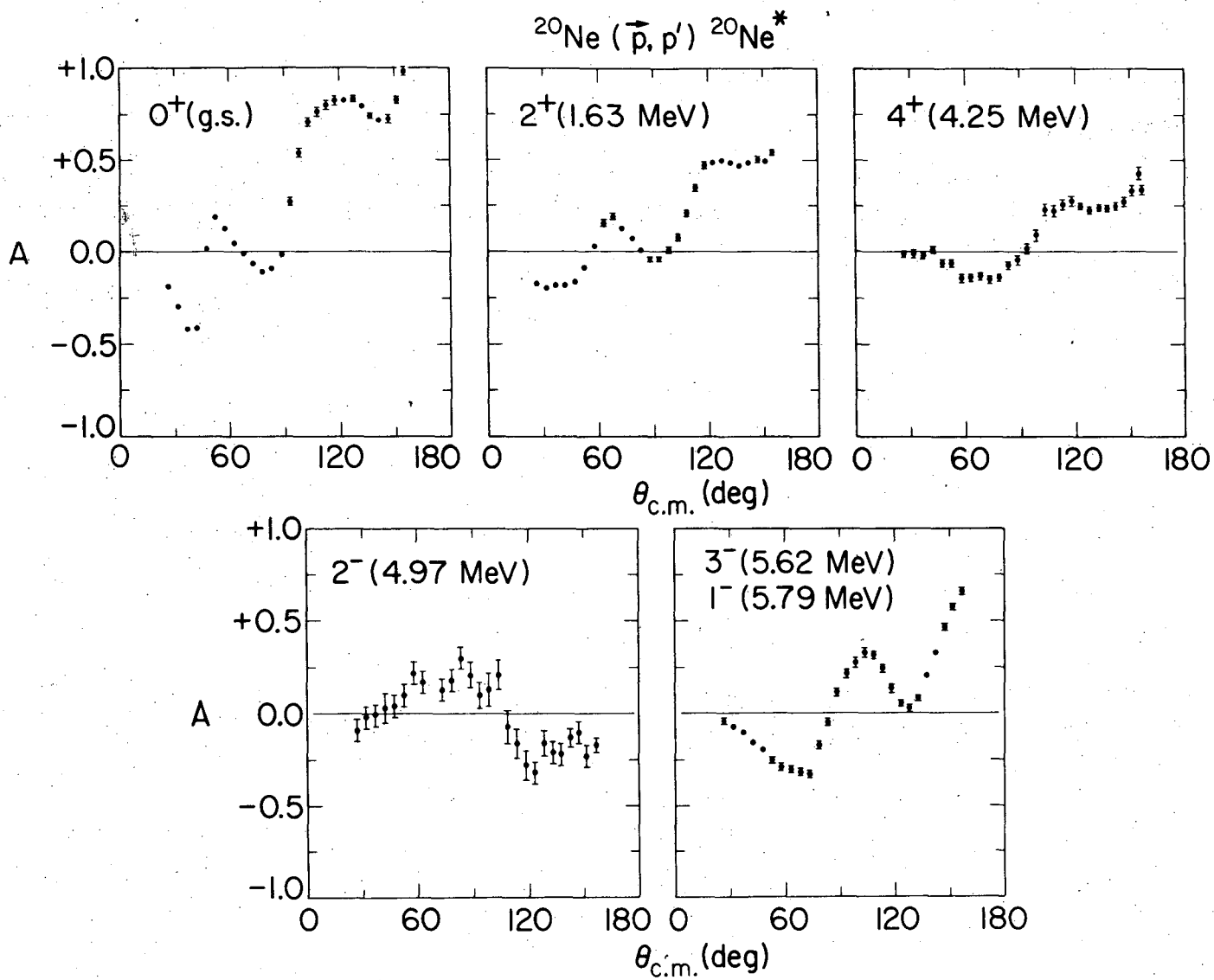
Figure 10 Coupled-channels calculations for the cross sections and analyzing power for the 2^+ and 4^+ states in ^{28}Si with full Thomas form. Optical model parameters of Table 2 were used. For the rotational model: — $\beta_2 = +0.40$, $\beta_4 = -0.10$; --- $\beta_2 = +0.40$, $\beta_4 = 0.00$; for the vibrational model: — x — x. The cross section data are from ref. 14.

Figure 11 Coupled-channels calculations for the analyzing powers and cross sections (rotational model) for the ground state $K = 0^+$ band in ^{28}Si with the full Thomas form. Optical model parameters of Table 2 were used. Where $\beta_{\text{LS}}^{\text{r}} = \beta_{\text{central}}^{\text{r}}$, — $\beta_2 = -0.40$, $\beta_4 = 0.10$. Where $\beta_{\text{LS}} = \beta_{\text{central}}$, — x — x $\beta_2 = -0.40$, $\beta_4 = 0.10$; and — · — $\beta_2 = -0.40$, $\beta_4 = 0.00$. The cross section data are from ref. 14.

Figure 12 Coupled-channels calculations for the first 0^+ , 2^+ , states in ^{32}S using the full Thomas form with $\beta_{\text{LS}} = \beta_{\text{central}}$ and a rotational model with $\beta_2 = +0.30$ (— · —) or -0.30 (—) and optical parameters of Table 2.

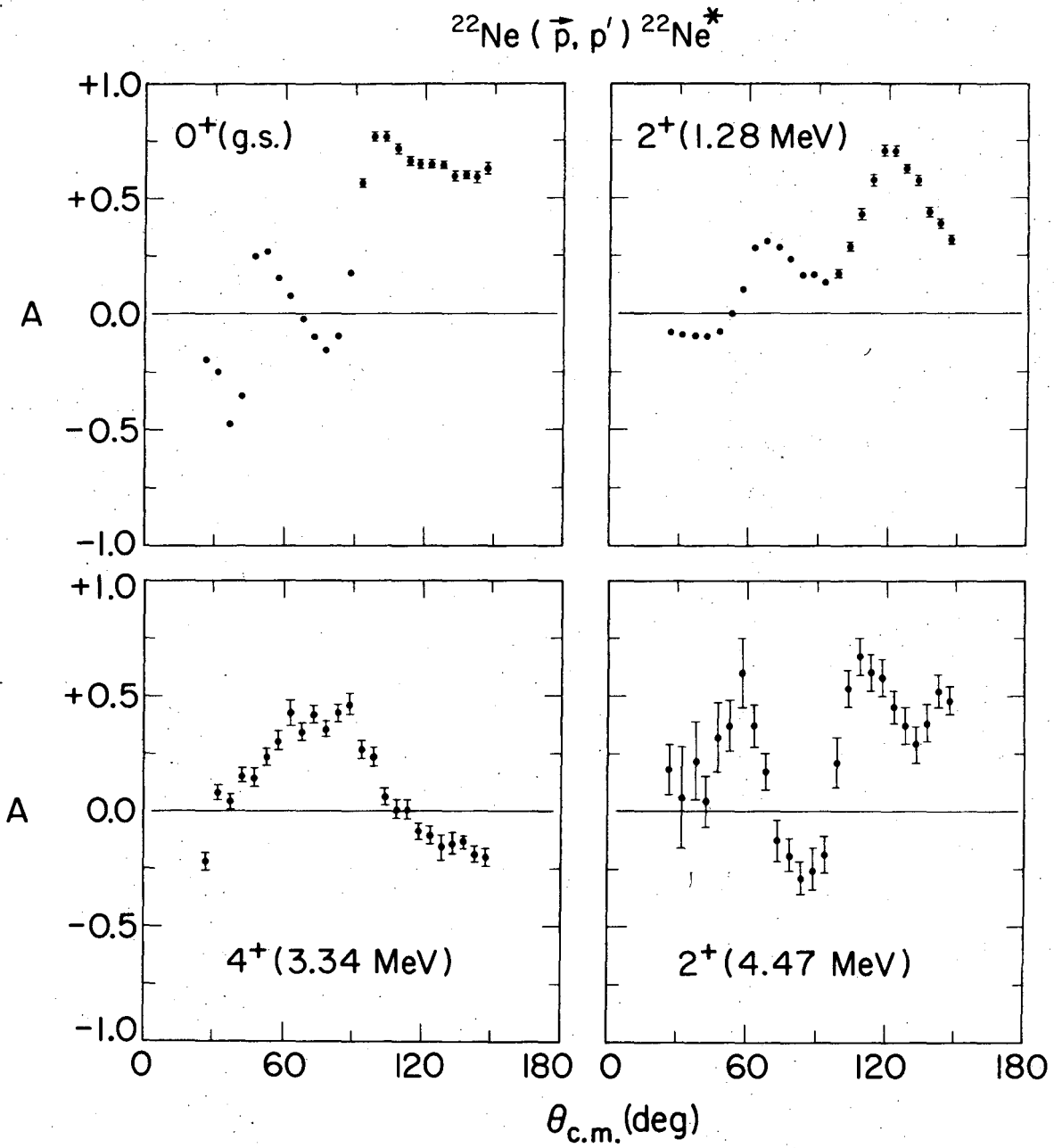
Figure 13 Coupled-channels calculations for the analyzing powers and cross sections for the strongly low-lying excited states in ^{32}S using a vibrational model, the full Thomas form with $\beta_{\text{LS}} = \beta_{\text{central}}$ and optical model parameters of Table 2. Calculations were done by coupling either the 0^+ , 2^+ (—) or the 0^+ , 2^+ , 3^- (— · —) states. Deformation parameters of 0.30 for the 2^+ , and 0.41 for the 3^- were used.

Figure 14 Coupled-channels calculations for the cross sections and analyzing power for the 2^+ and 3^- states in ^{16}O using the full Thomas form and the vibrational model. We used the optical model parameters of Table 2 with $\beta_2 = +0.20$ and $\beta_3 = +0.50$. — $\beta_{\text{LS}} = \beta_{\text{central}}$, - - - $\beta_{\text{LS}} = \text{twice } \beta_{\text{central}}$. The analyzing power data are from the present work at 30.3 MeV, while the cross-section data are from ref. ²³) at 29.81 MeV.



XBL 756-3217

Fig. 1



XBL 756-3218

Fig. 2

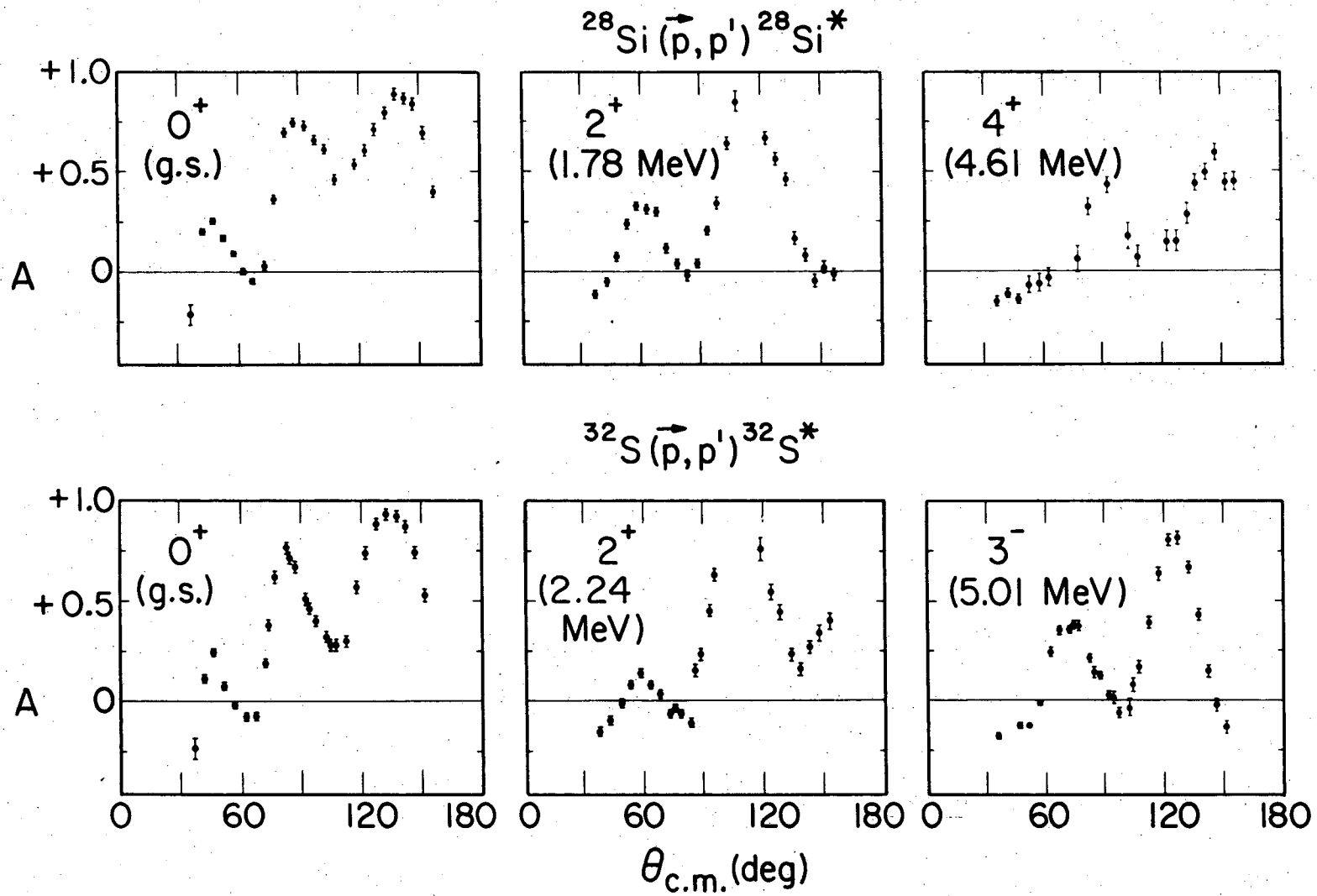
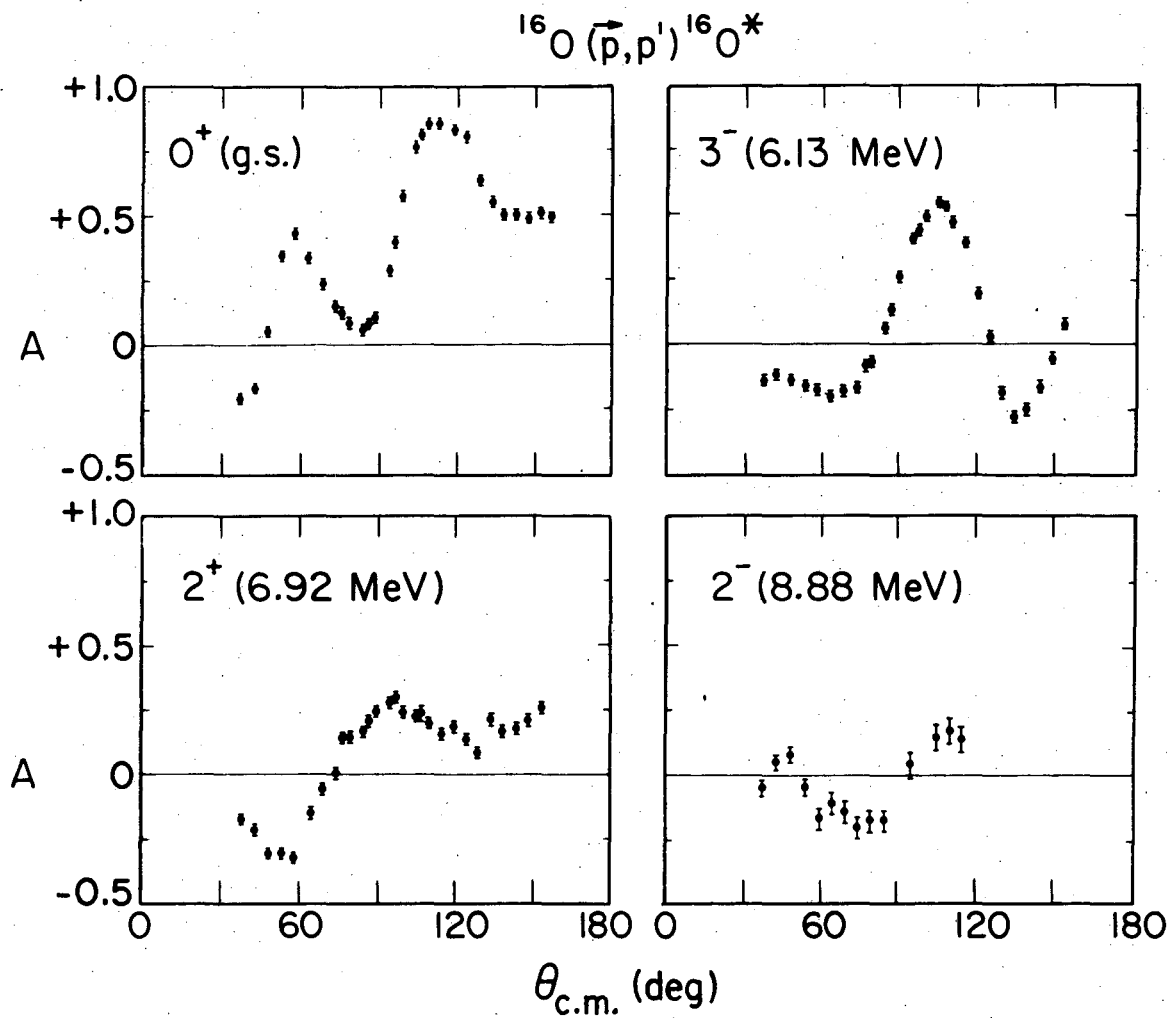
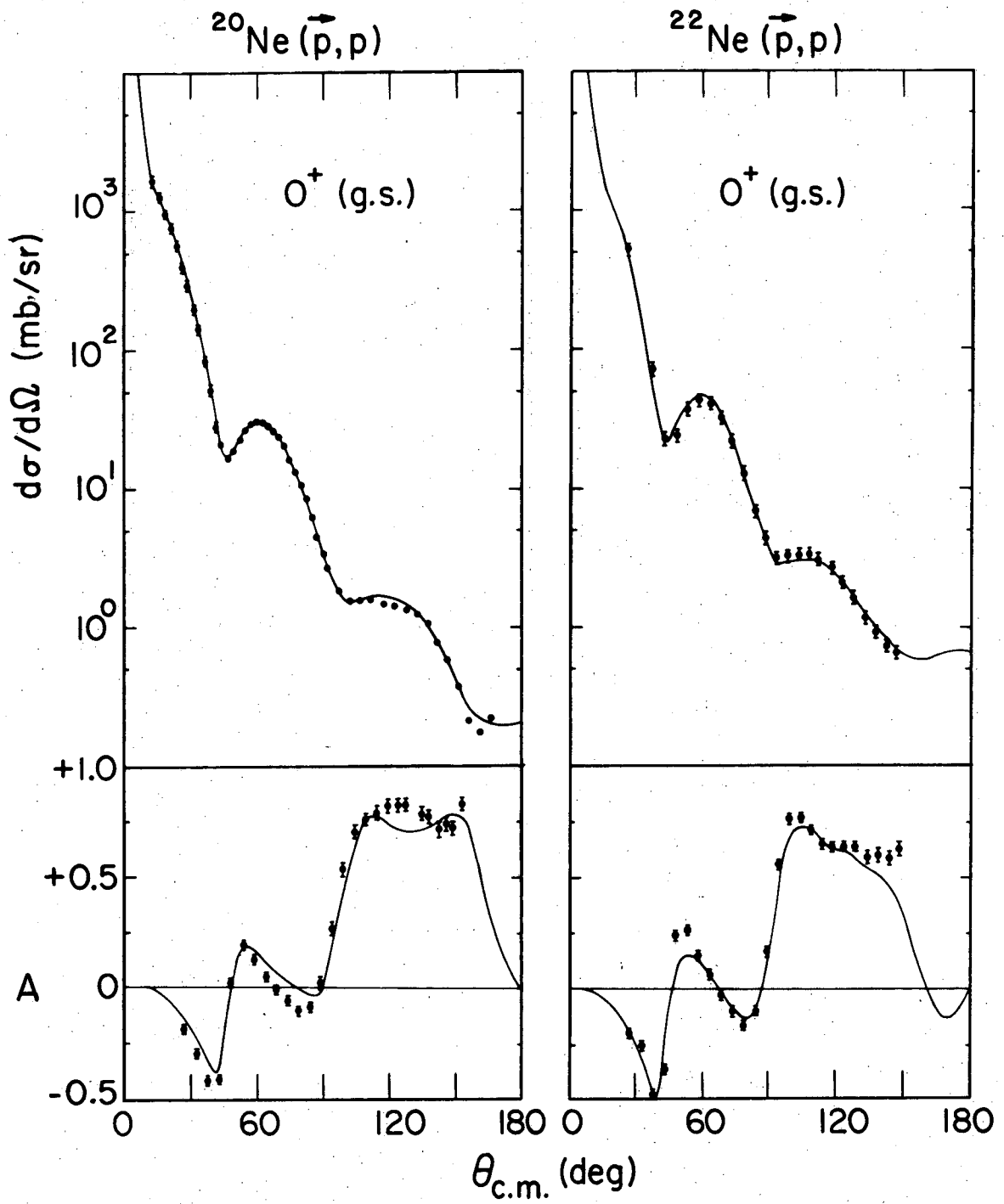


Fig. 3



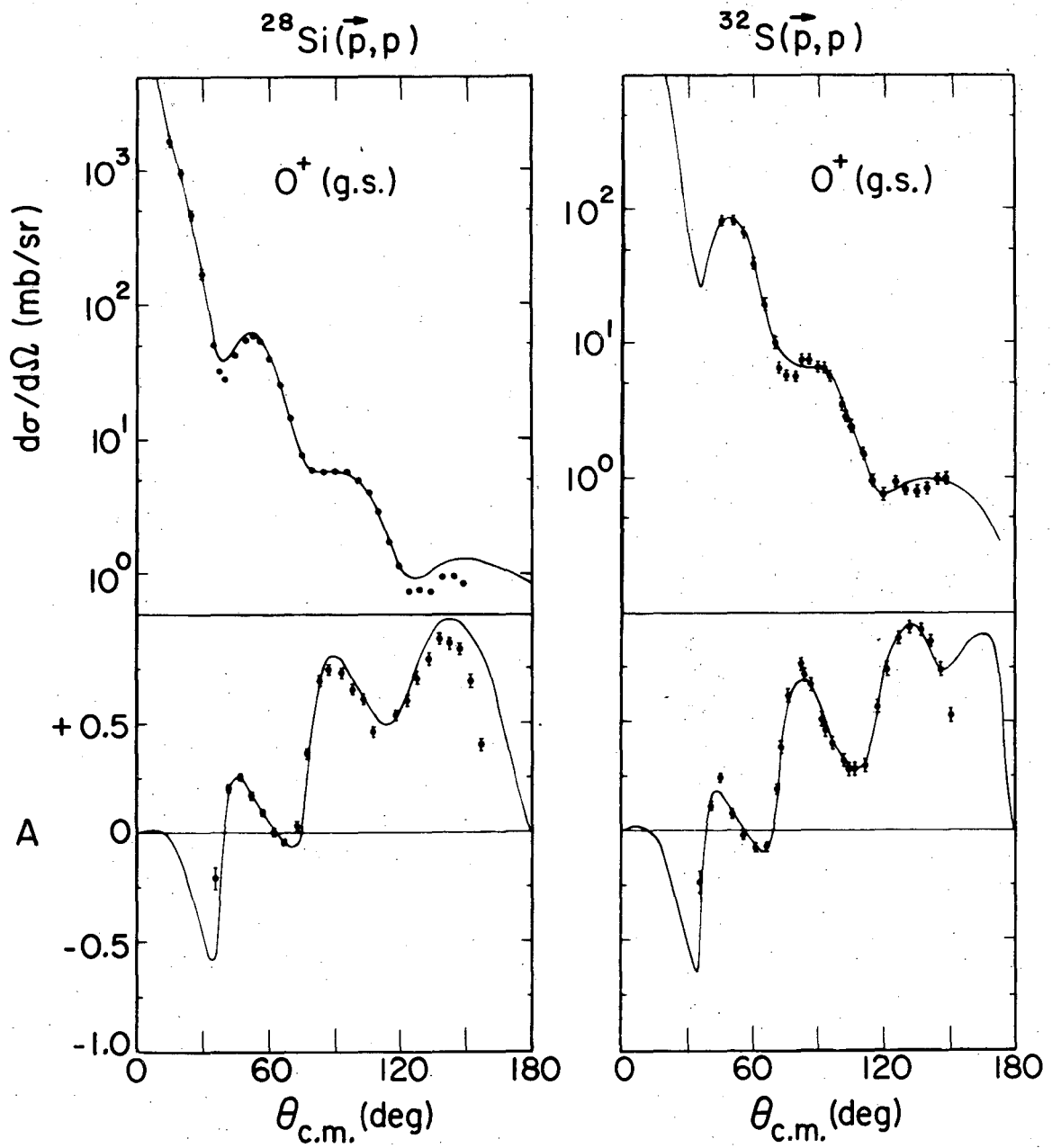
XBL 756-3220

Fig. 4



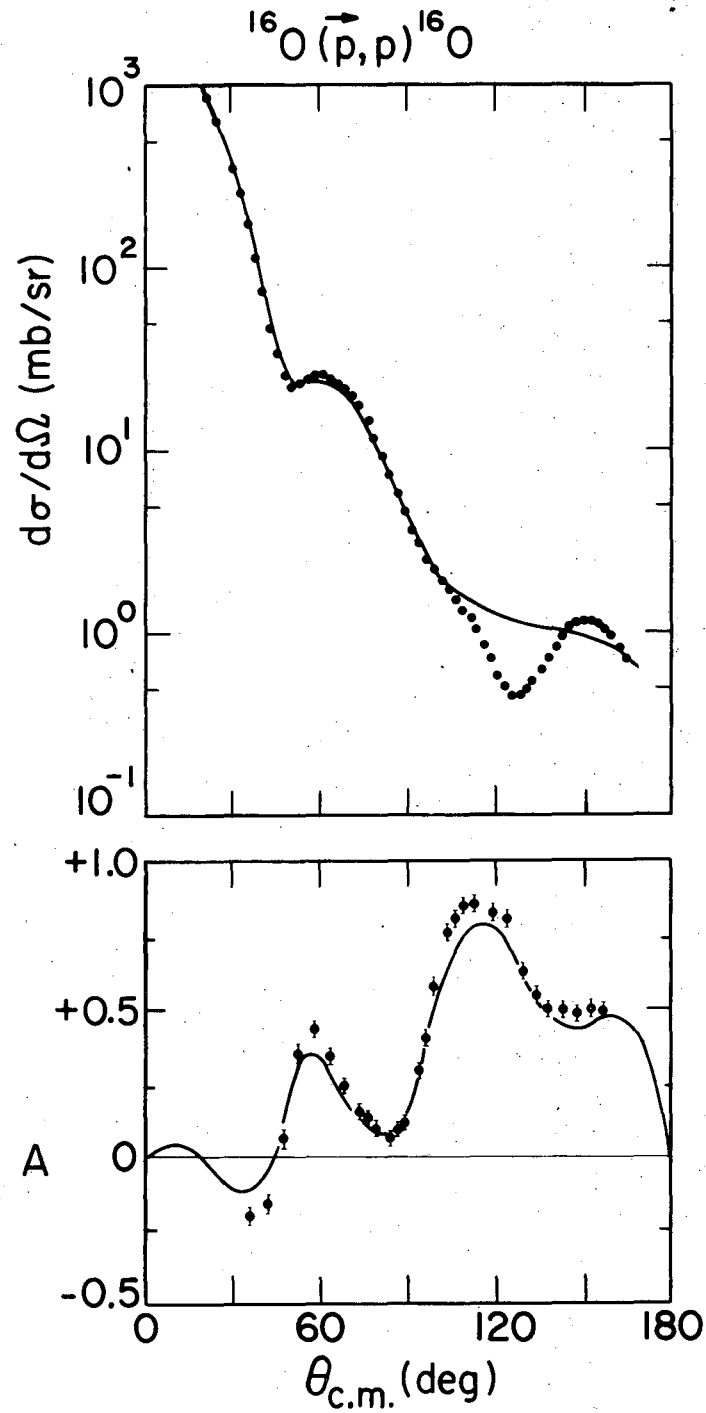
XBL 756-3221

Fig. 5



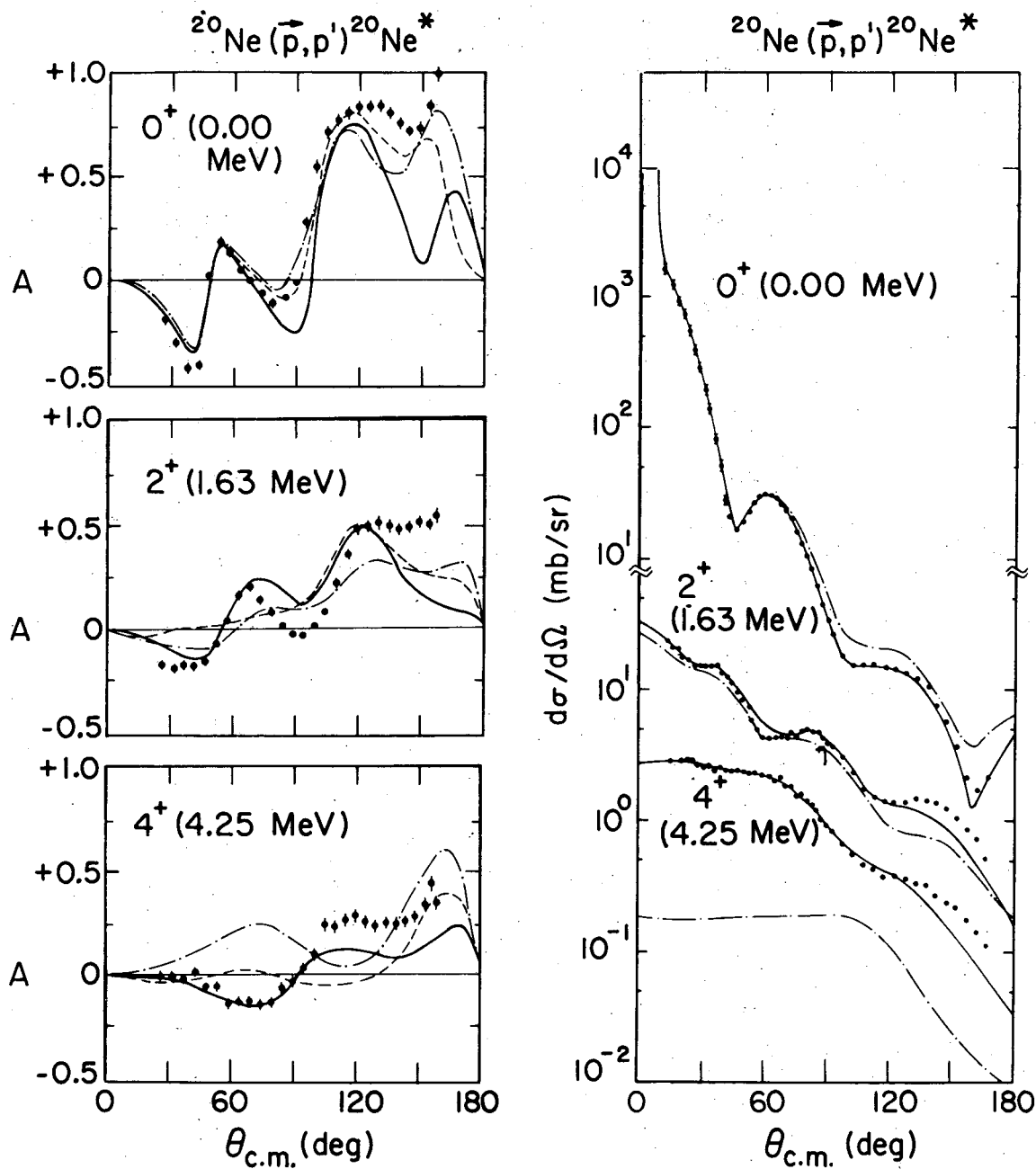
XBL 756-3222

Fig. 6



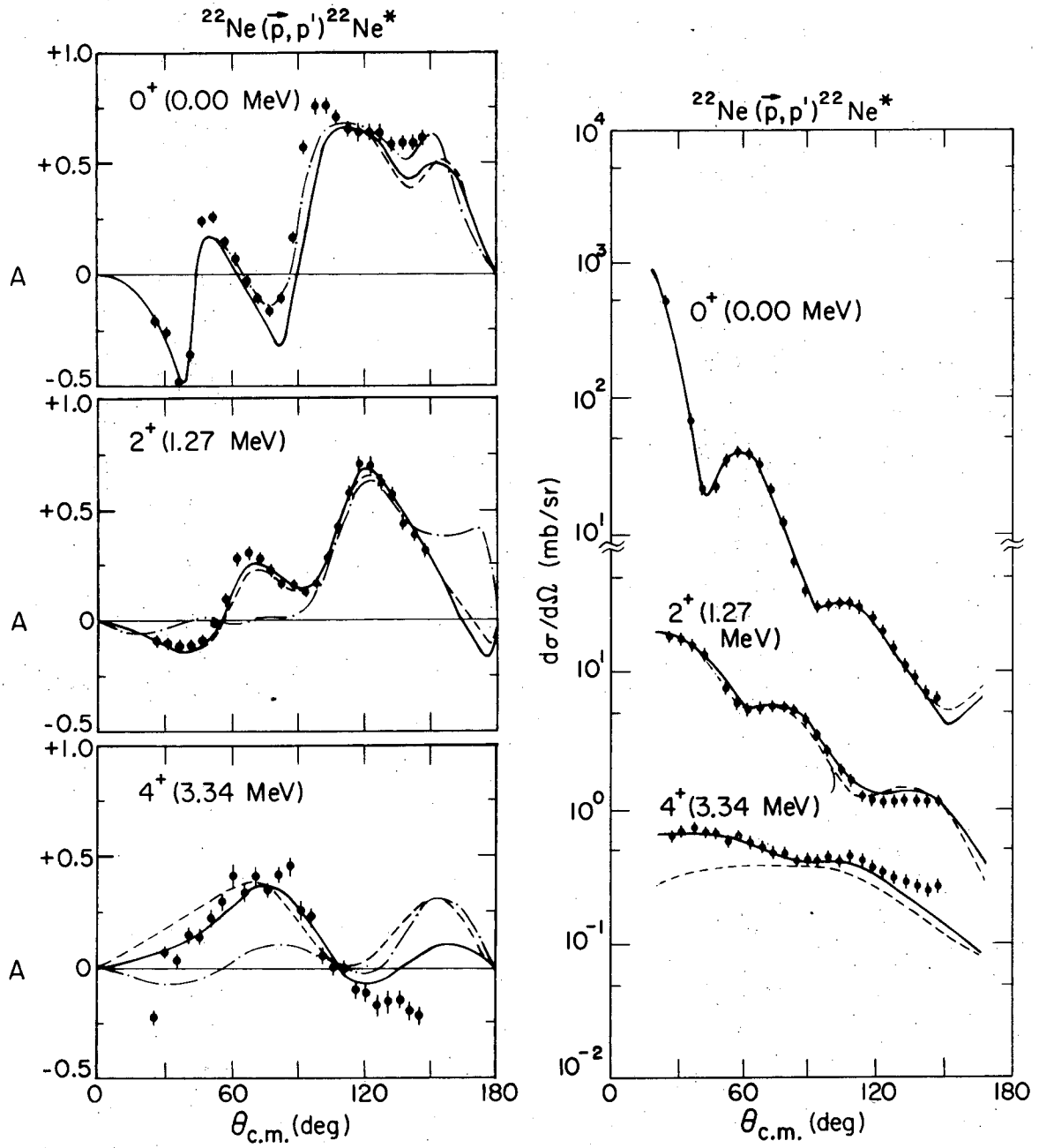
XBL 756-3223

Fig. 7



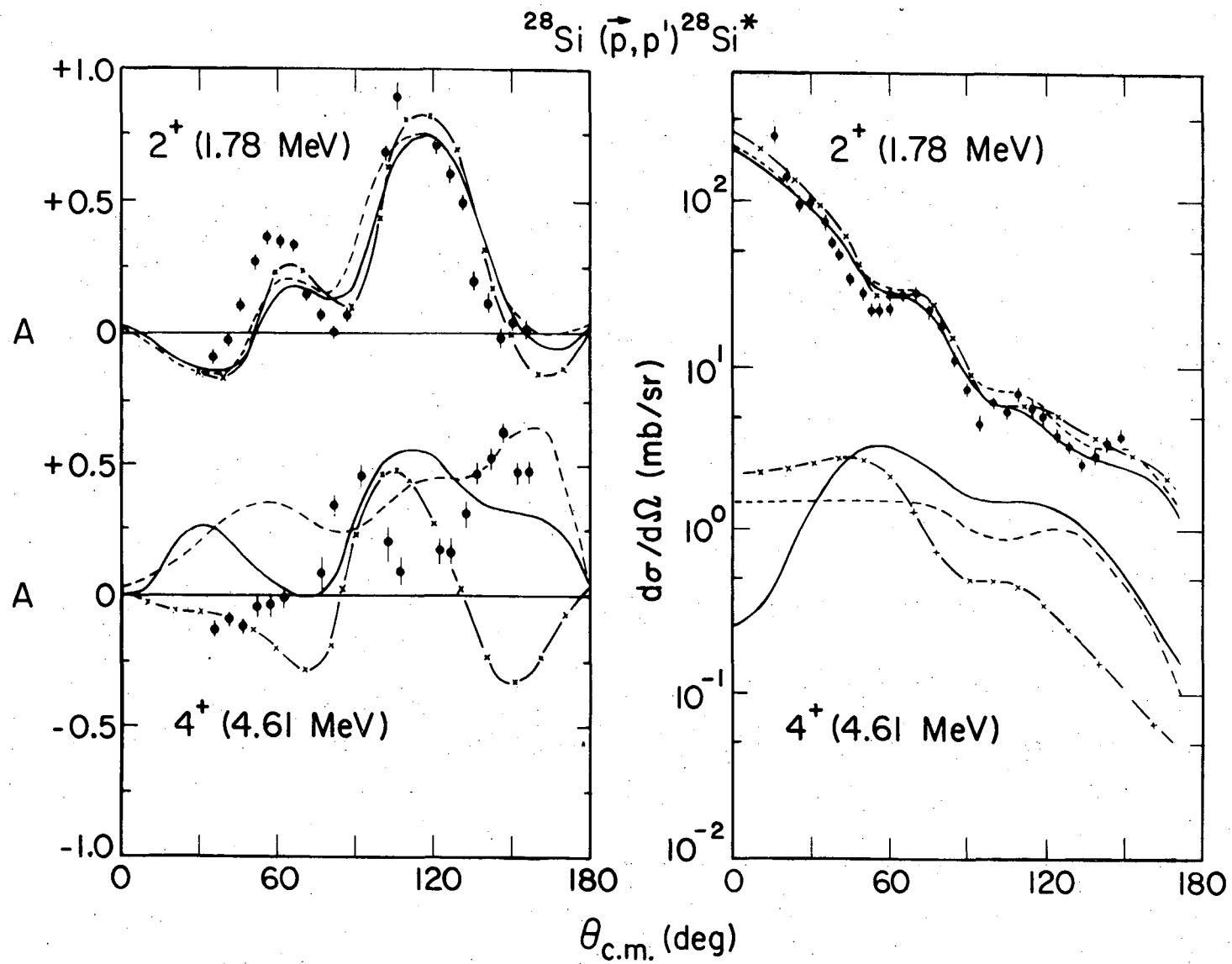
XBL 756-3224

Fig. 8



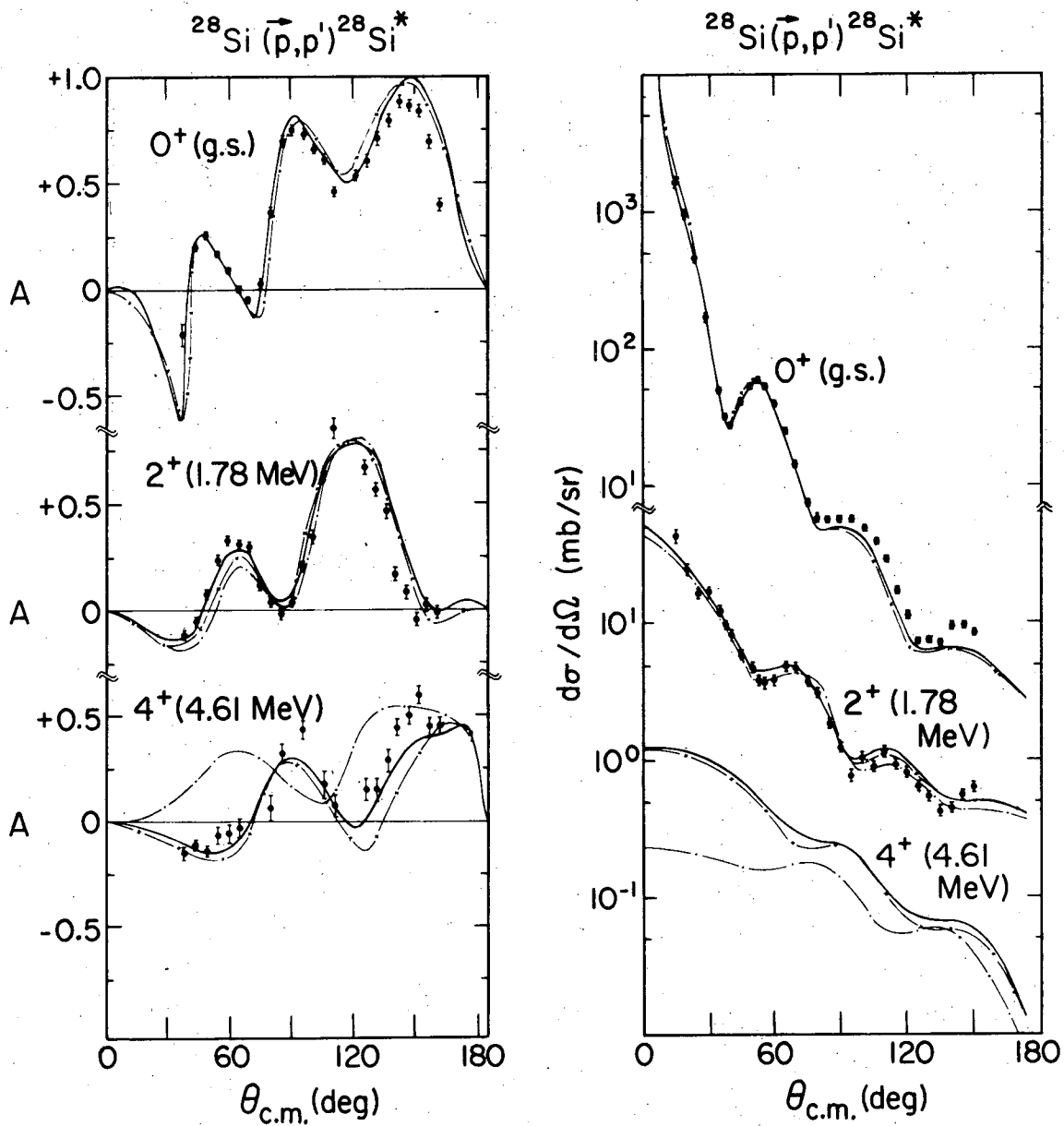
XBL 756-3225

Fig. 9



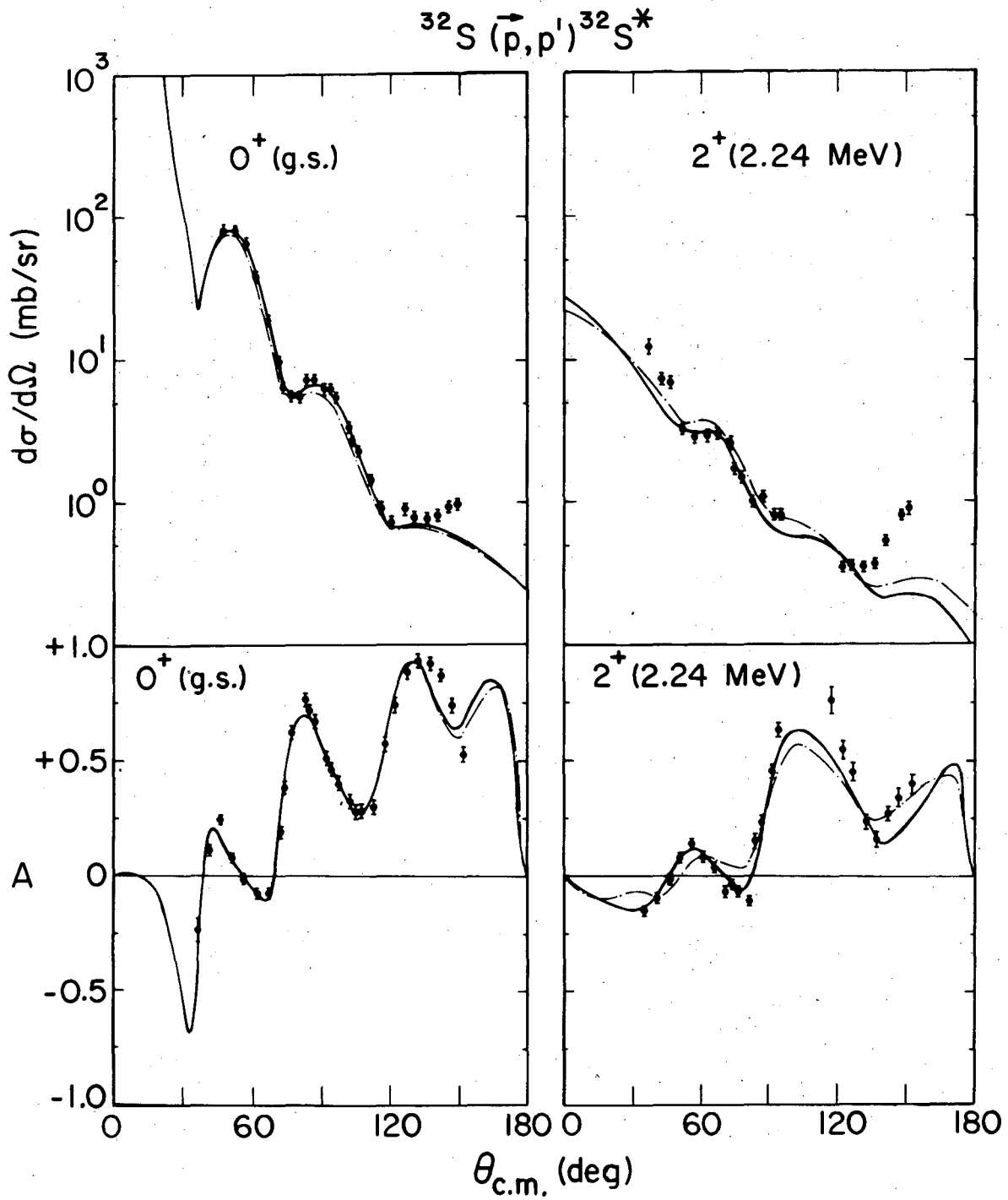
XBL 756-3226

Fig. 10



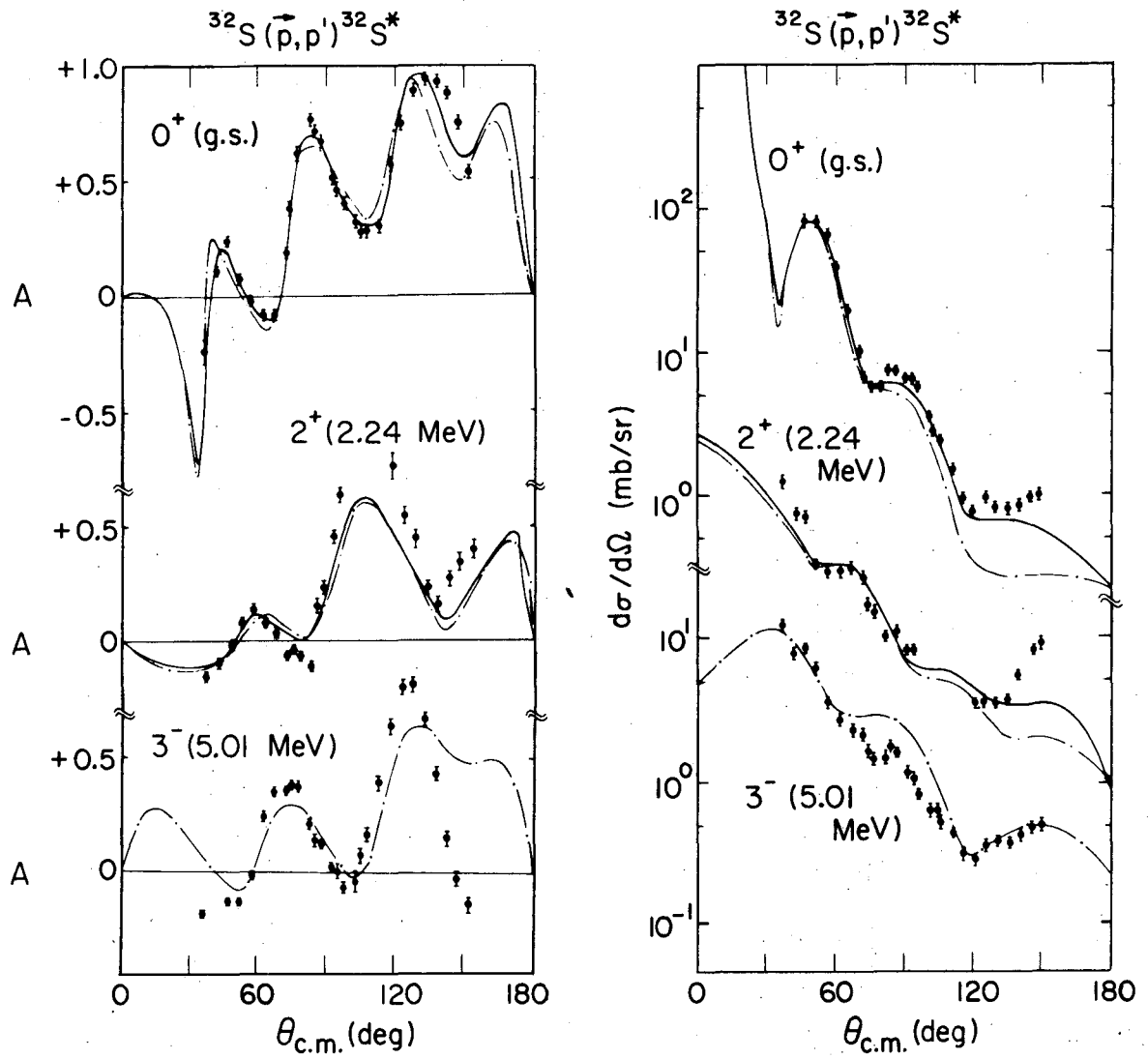
XBL 756-3227

Fig. 11



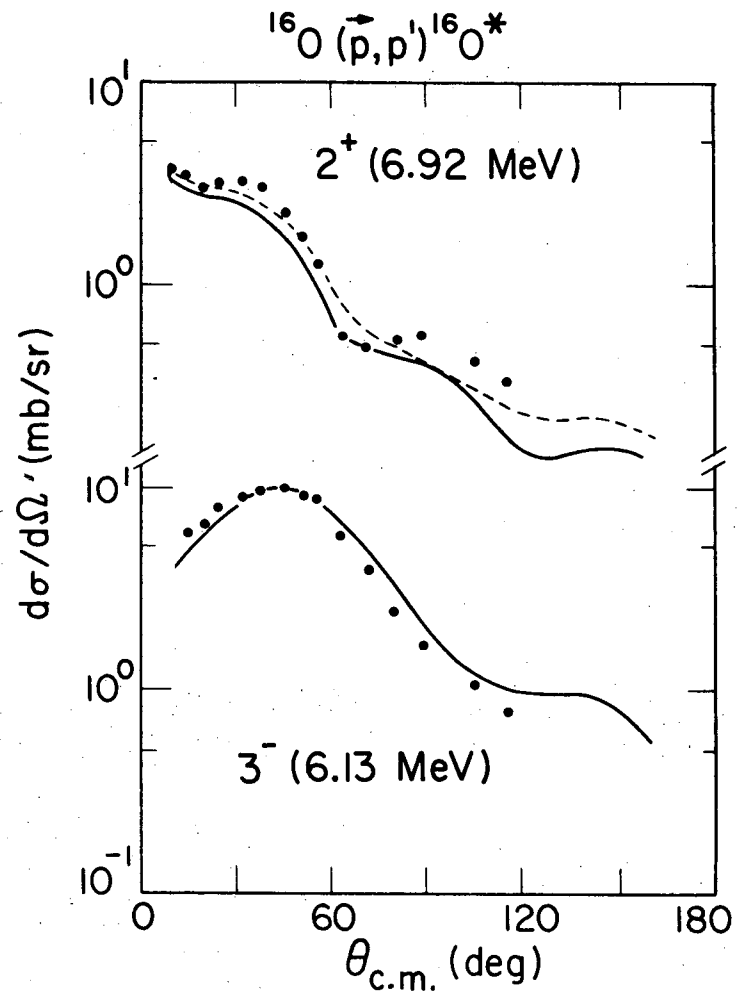
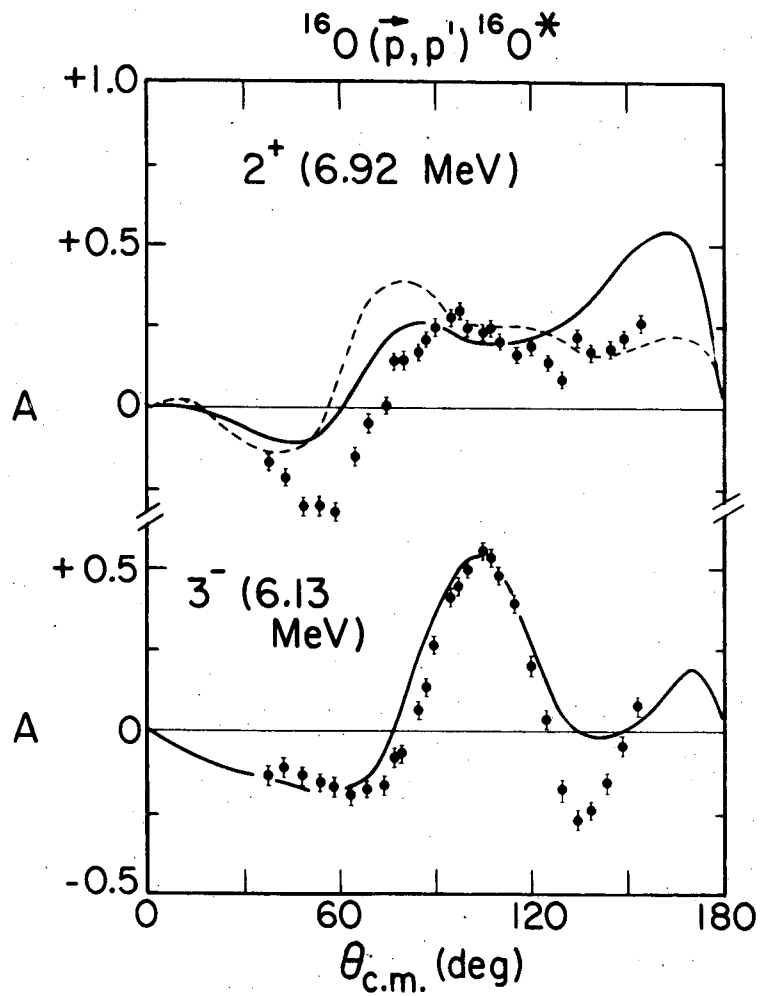
XBL 756-3228

Fig. 12



XBL 756-3229

Fig. 13



XBL 756-3230

Fig. 14

LEGAL NOTICE

This report was prepared as an account of work sponsored by the United States Government. Neither the United States nor the United States Energy Research and Development Administration, nor any of their employees, nor any of their contractors, subcontractors, or their employees, makes any warranty, express or implied, or assumes any legal liability or responsibility for the accuracy, completeness or usefulness of any information, apparatus, product or process disclosed, or represents that its use would not infringe privately owned rights.

TECHNICAL INFORMATION DIVISION
LAWRENCE BERKELEY LABORATORY
UNIVERSITY OF CALIFORNIA
BERKELEY, CALIFORNIA 94720